N O T I C E

THIS DOCUMENT HAS BEEN REPRODUCED FROM MICROFICHE. ALTHOUGH IT IS RECOGNIZED THAT CERTAIN PORTIONS ARE ILLEGIBLE, IT IS BEING RELEASED IN THE INTEREST OF MAKING AVAILABLE AS MUCH INFORMATION AS POSSIBLE

PRINCETON UNIVERSITY
School of Engineering and Applied Science
Department of Mechanical and Aerospace Engineering

"TURBULENCE MEASUREMENTS IN HIGH-SPEED FLOWS BY RESONANT FLUORESCENCE"

Final Report

for

Grant NSG 2366

1/1/79 to 12/31/81

ORIGINAL CONTAINS COLOR ILLUSTRATIONS

Principal Investigator:
Richard B. Miles
Department of Mechanical and Aerospace Engineering
Princeton University
Princeton, New Jersey 08544

MAE Report No. 1565

(NASA-CR-168934) TURBULENCE MEASUREMENTS IN HIGH-SPEED FLOWS BY RESONANT FLUORESCENCE Final Report, 1 Jan. 1979 - 31 Dec. 1981 (Princeton Univ., N. J.) 30 p HC A03/MF A01 CSCL 20D G3/34

N82-24447

Unclas 09962

NASA/AMES RESEARCH CENTER
Moffett Field, California

MAY 1982 RECEIVED NASA STI FACILITY ACCESS DEPT.

May 1982

ABSTRACT

Both mean flow and turbulence measurements have been investigated using the Resonant Doppler Velocimeter in a Mach 3.2 nitrogen flow. Data is presented showing velocity, temperature and pressure measured point by point across the flow field. This data is compared with conventional pitot and temperature surveys. Turbulence was induced by a small metal tab in the flow and observed by both hot wire and RDV techniques. Photographs of the flow field demonstrate the utility of the RDV for quantitative flow field visualization.

I. TECHNICAL DISCUSSION

A. Introduction

The Resonant Doppler Velocimeter (RDV) was proposed by R.B. Miles in 1975[1,2] and demonstrated in hypersonic helium flow by M. Zimmermann and R. B. Miles.[3,4,5,6] This final report describes the recent development of the RDV for free stream and turbulence measurements in a supersonic nitrogen jet.

Basically, the RDV is a Laser Induced Fluorescence (LIF) technique. In this particular investigation, sodium atoms were used as tracer particles. By tuning a narrow linewidth dye laser through the absorption range of the sodium D_2 line, the frequency and lineshape of these seeded sodium atoms can be obtained. Then, from the Doppler shift of the spectral lines, one can calculate the flow velocity. From the spectral lineshape, the static temperature and the static pressure can be derived.

Since an atomic species is used as a tracer, the particle lag problem, which hinders the application of Laser Doppler Velocimetry (LDV) in supersonic flow, is avoided. The atomic species can follow the turbulent motion of the flow, thus, the RDV can be applied for turbulent measurements as well as for the measurements of the mean flow properties. The LIF nature of the technique makes RDV an excellent point measurement technique. Furthermore, by taking advantage of the high fluorescence intensity of the sodium atoms, it can be used for flow visualization.

B. Experiment Configuration

The experimental setup is shown schematically in Figure 1. The nitrogen jet was generated by expanding room temperature nitrogen gas through a

Mach 3.2 nozzle. A small amount of sodium vapor was injected through a heated needle centered 0.5 inch upstream of the throat of the nozzle. Some flow properties of the jet are tabulated in Table 1. The heat required to vaporize the sodium was provided by a small oven. The small amount of purge nitrogen which flowed through the oven and the needle was heated to several hundred degrees centigrade. Hence the jet had a total temperature around 70°C.

The dye laser was a Spectra Physics model-580 single-frequency tunable laser modified to include a dye jet stream and pumped by a Coherent Radiation model-53A argon ion laser. The output was split into several beams for laser intensity stabilization, frequency selection, and other monitoring functions as well as data collection. A monochromator and a hot sodium cell were used to position the dye laser frequency at the sodium D_2 line. An optical spectrum analyzer was used to check the mode structure of the dye laser and to calibrate the laser frequency. The laser intensity was monitored by a photodiode. Frequency reference for the velocity measurement was provided by an atomic beam device. The probe beam intersected the supersonic jet at an angle and excited the sodium atoms seeded in the flow.

Four channels of data were sampled by an HP1000 mini-computer system through a Preston model GMAD/1 A-D converter. 256 data points were sampled sequentially as the laser was tuned in discrete steps. The raw data of a typical experiment is shown in Figure 2. The fluorescence signal gives the broadened and shifted absorption profile of the sodium in the nitrogen and is characteristic of the mean properties of the flow.

C. Data Processing

The spectrum in Figure 2 was then least-squares fitted to a Voigt profile. The fitted result is shown in Figure 3. The abscissa is the relative laser frequency in MHz and the ordinate is the fluorescence intensity in arbitrary units. The crosses in the figure represent the experimental absorption spectrum, while the solid line through the crosses is the computer-generated theoretical sodium D_2 line which is the best least-squares fit to the experimental result. The sodium D_2 line is in fact a superposition of six hyperfine lines weighed differently in their intensities. The hyperfine structure is shown by the vertical bars in the spectrum. Five parameters were used in the fitting process. They are the spectral intensity for $3^2S_{1/2}$, $F = 2$ to $3^2P_{2/3}$, $F = 3$ transition; the background intensity, the frequency half width at half maximum (HWHM) of the Voigt profile, the ratio of the line widths of the Lorentzian profile and Gaussian profile, and the frequency shift relative to the reference Doppler-free sodium D_2 line. From the last three parameters, one can derive the pressure, temperature, and velocity of the jet.

The data analysis is complicated by the fact that in a sodium-nitrogen system, pressure shift and quenching and collision broadening effects cannot be neglected. In order to get accurate velocity measurement, the pressure shift collision cross section must be found. Similarly, pressure measurements rely on the knowledge of the quenching and collision broadening cross section. These cross sections are not well documented in the literature for the lower temperature in the jet.

Both the shift and broadening cross sections can be measured by intersecting the probe laser beam with the ideally expanded jet at 90°. Since

the jet is ideally expanded, the static pressure is uniformly distributed across the jet. Thus from the static pressure measured with a pitot probe and the quenching and collision broadening linewidth obtained from curve fitting, one can calculate the broadening cross section. Since the laser beam intersects the jet at 90°, there is no Doppler shift. Thus, if there is any shift in frequency, it is caused by the pressure shift effect. From the measured frequency shift, temperature, and pressure, the pressure shift cross section can be determined.

D. Experimental Results

Since the static temperature is not uniform across the jet, the temperature dependence of the broadening and pressure shift cross sections can be obtained by moving the probe point across the jet. The results of these measurements are presented in Figure 4. Assuming the temperature dependences of these cross sections are in the form:

$$\sigma_q = k_q T^{\alpha}$$

$$\sigma_s = k_s T^{\beta} ,$$

a least-squares curve fitting of α and β yields -0.302 ± 0.051 and -1.101 ± 0.272 respectively.

After the cross sections were determined, a measurement across an ideally expanded jet was made with an intersecting angle of $127.5° \pm 0.3$. The measured velocity, temperature, pressure, and Mach number profiles are shown in Figures 5 through 8. The velocity and Mach number profiles can be compared with the profiles obtained from a pitot survey across the same jet (Figures 9 and 10). The velocity measured with RDV at the center of the jet is about 700 m/sec which is about 20 m/sec higher than that

calculated from the pitot pressure. The differences become larger at the edges of the jet. This discrepancy has not yet been resolved but it may be attributable to the large uncertainty in the measured temperature dependence of the pressure shift cross section.

A similar trend can be seen in Mach number distribution when compared with the calculated results from pitot survey. The variations from the calculated Mach numbers are due to the uncertainties in the measured temperature. The uncertainty for the temperature measurement is about $\pm 20°K$. Similarly the uncertainty in the pressure measurement is quite large; it is about ± 1.5 torr.

Temperature and pressure uncertainties are mainly due to the limited scanning of the dye laser frequency. The dye laser can be tuned linearly for 5 GHz. Yet the HWHM of the Voigt profile varies from 600 MHz at the center of the jet to 750 MHz at the edge of the jet. Thus, the scanning range is only about 4 times the spectral linewidth. Due to the importance of the tails of the distribution, the accuracy will increase substantially with a larger scan width.[7] Nevertheless, though the precisions of the temperature and pressure measurements are not very good, they generally agree with the pitot probe and total temperature measurements.

The pitot pressure measured outside of the jet was 12.7 psi and the pressure obtained from the RDV was also around 12 psi. The total temperature calculated from the relation

$$T^t = \frac{V^2}{2C_p} + T$$

is presented in Figure 11. This can be compared with the total temperature profile measured by a thermocouple and corrected with a recovery coefficient of 0.95 (Figure 12).

To demonstrate that the RDV can be applied for turbulent measurements, the photomultiplier was operated in the voltage mode. The fluorescence signals were sampled through GMAD/1 with a sampling rate of 50 KHz. More than 20,000 data points were sampled each time and the frequency spectrum was obtained through the fast Fourier transformation of this data. Figure 13 is the frequency spectrum obtained this way. It can be compared with the frequency spectrum derived from hot wire signal (Figure 14). However, even though these two spectrum look the same, there is no noticeable frequency structure in the free jet. In order to more convincingly demonstrate the measurement capability of the RDV in a turbulent flow, a thin metal tab was introduced into the jet to generate large scale eddies. Figure 15 is the laser frequency spectrum from the fluorescence signal after the metal piece was introduced into the jet. A peak at 400 Hz can be clearly seen. The same peak can be found in the corresponding frequency spectrum from hot wire signal (Figure 16).

Flow visualization was also demonstrated in an underexpanded nitrogen jet. The laser was expanded with a cylindrical beam expander into a sheet of light. Then this light sheet was directed at a small angle against the jet (as shown in Figure 17). Due to the mismatch of the jet pressure and the ambient pressure, a diamond-shaped structure was formed as depicted in Figure 17. When this structure was illuminated with the laser light sheet, only a portion of the jet with proper velocity will fluoresce. This feature can be clearly seen in the photograph shown in Figures 18 and 19. Figure 18 shows the low velocity components of the jet. The narrow illuminated region downstream shows only faint structure because the laser was not focused to a sheet. Some background fluorescence can also be seen due to the ambient

gas. Figure 19 is a picture of the same jet with the laser tuned to highlight the high velocity components. Note that the low velocity regions are now dark and the high velocity regions are bright. Some asymmetry can also be observed indicating that the flow velocities are not always parallel to the centerline.

E. Conclusion

This work demonstrates that RDV is a tool for flow diagnostics in a supersonic nitrogen jet. It is not only good for average and turbulent point measurements but also useful for flow visualization. Due to the relatively high flow temperature and pressure, the laser scanning range has to be expanded before more accurate results can be obtained from the RDV measurements. Also the pressure shift cross section and its temperature dependence will affect the accuracy of velocity measurements. Two-beam experiments as described in Ref. 6 should give more reliable measurements of the pressure shift cross sections. In order to conduct two-beam experiments in this system, a larger scanning range of the laser frequency will be required.

F. References

1. R.B. Miles, "Resonant Doppler Velocimeter", AGARD CP-193, Paper 19-1, 1976.

2. R.B. Miles, "Resonant Doppler Velocimeter", Phys. of Fluids, Vol. 18, No. 6, p. 751, June 1975.

3. R.P. Miles, E. Udd, and M. Zimmermann, "Quantitative Flow Visualization in Sodium Vapor Seeded Hypersonic Helium", Appl. Phys. Lett. 32(5), March 1978.

4. M. Zimmermann and R.B. Miles, "Hypersonic Helium Flow Measurements with the Resonant Doppler Velocimeter", Appl. Phys. Lett. 37(8), November 1980.

5. M. Zimmermann and R.B. Miles, "Low Temperature He-Na Collision Rate Measurement", J. Phys. B: Atom. Molec. Phys., Vol. 14, L85, 1981.

6. M. Zimmermann, "Resonant Doppler Velocimeter", Ph.D. Thesis, Princeton University, March 1980.

7. M. Zimmermann, to be published.

II. PUBLICATIONS AND PRESENTATIONS PREPARED UNDER THIS GRANT

Publications

M. Zimmermann and R.B. Miles, "Hypersonic Helium Flow Field Measurements with the Resonant Doppler Velocimeter", Appl. Phys. Lett. 37, November 1980, p. 885.

M. Zimmermann and R.B. Miles, "Low Temperature Helium-Sodium Collision Rate Measurements", J. of Physics B14, February 1981, p. L85.

Presentations

M. Zimmermann and R.B. Miles, "Measurement of Hypersonic Helium Flow Properties with the Resonant Doppler Velocimeter", 1979 IEEE/OSA Conference on Laser Engineering and Applications, Washington, D.C., May-June 1979. IEEE Journal of Quantum Electronics, QE-15, paper 3.7, September 1979, p. 18D.

M. Zimmermann, S. Cheng and R.B. Miles, "Measurements of Supersonic Nitrogen Flow Properties with the Resonant Doppler Velocimeter", 1981 IEEE/OSA Conference on Lasers and Electro-optics, Washington, D.C., June 1981. CLEO'81 Technical Digest, paper WO2, Washington, D.C.: Optical Society of America, 1980, p. 62.

M. Zimmermann, S. Cheng and R.B. Miles, "Characterization of a Free Supersonic Nitrogen Jet with the Resonant Doppler Velocimeter", 34th Meeting of the American Physical Society, Division of Fluid Mechanics, Monterey, CA, November 1981. Bulletin of the American Physical Society 26, Paper EH4, New York: American Institute of Physics, 1981, p. 1285.

M. Zimmermann, S. Cheng and R.B. Miles, "Flow Visualization in Supersonic Air with the Resonant Doppler Velocimeter", 1982 IEEE/OSA Conference on Lasers and Electro-optics, Phoenix, Arizona, April 1982. CLEO'82 Technical Digest, paper ThS4, Washington, D.C.: Optical Society of America, 1982.

III. PERSONNEL

R. B. Miles	Associate Professor
M. Zimmermann	Postdoctoral Associate
S. Cheng	Graduate Student
R. Bogart	Technician

Table 1

Stagnation Pressure	13 psi
Plenum Chamber Pressure	12.7 torr
Needle Temperature	650°C
Throat Diameter of the Nozzle	0.086 in.
Exit Diameter of the Nozzle	0.223 in.
Cone Angle of the Conical Nozzle	4°

ORIGINAL PAGE IS
OF POOR QUALITY

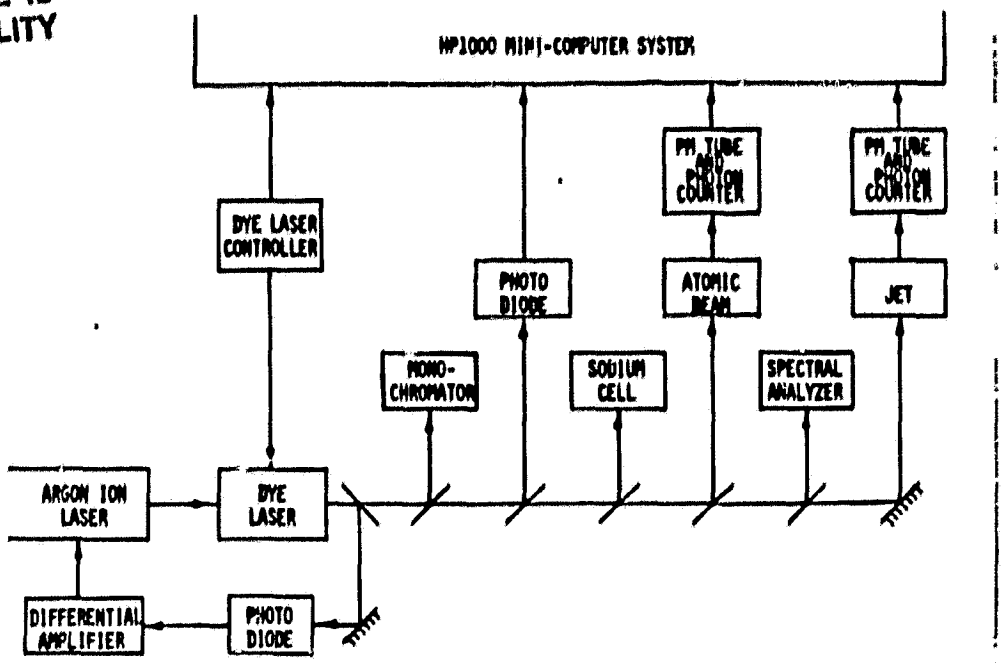

Figure 1a. Schematic diagram of the experimental setup for RDV.

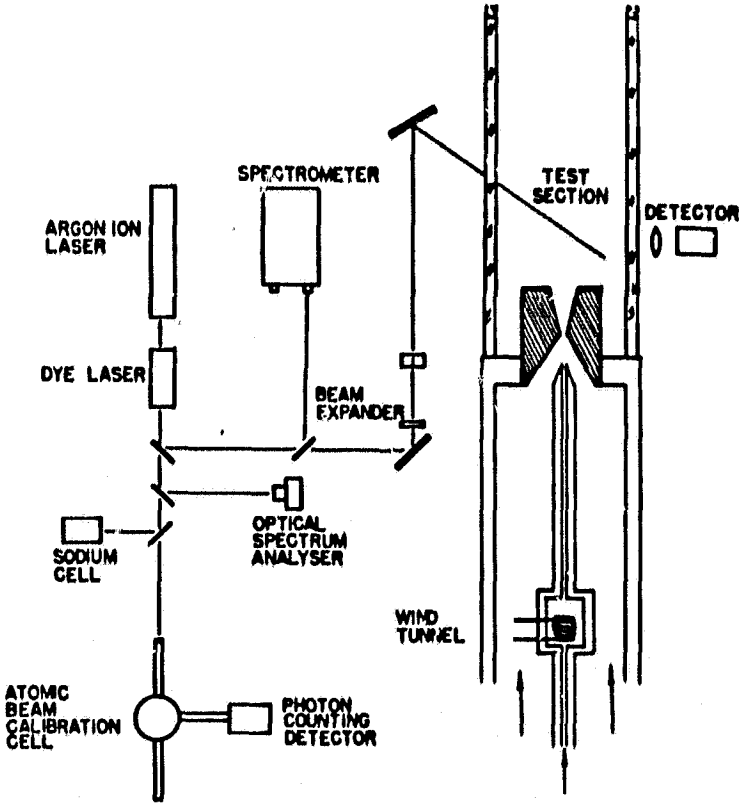

Figure 1b. The layout of the experimental setup.

ORIGINAL PAGE IS
OF POOR QUALITY

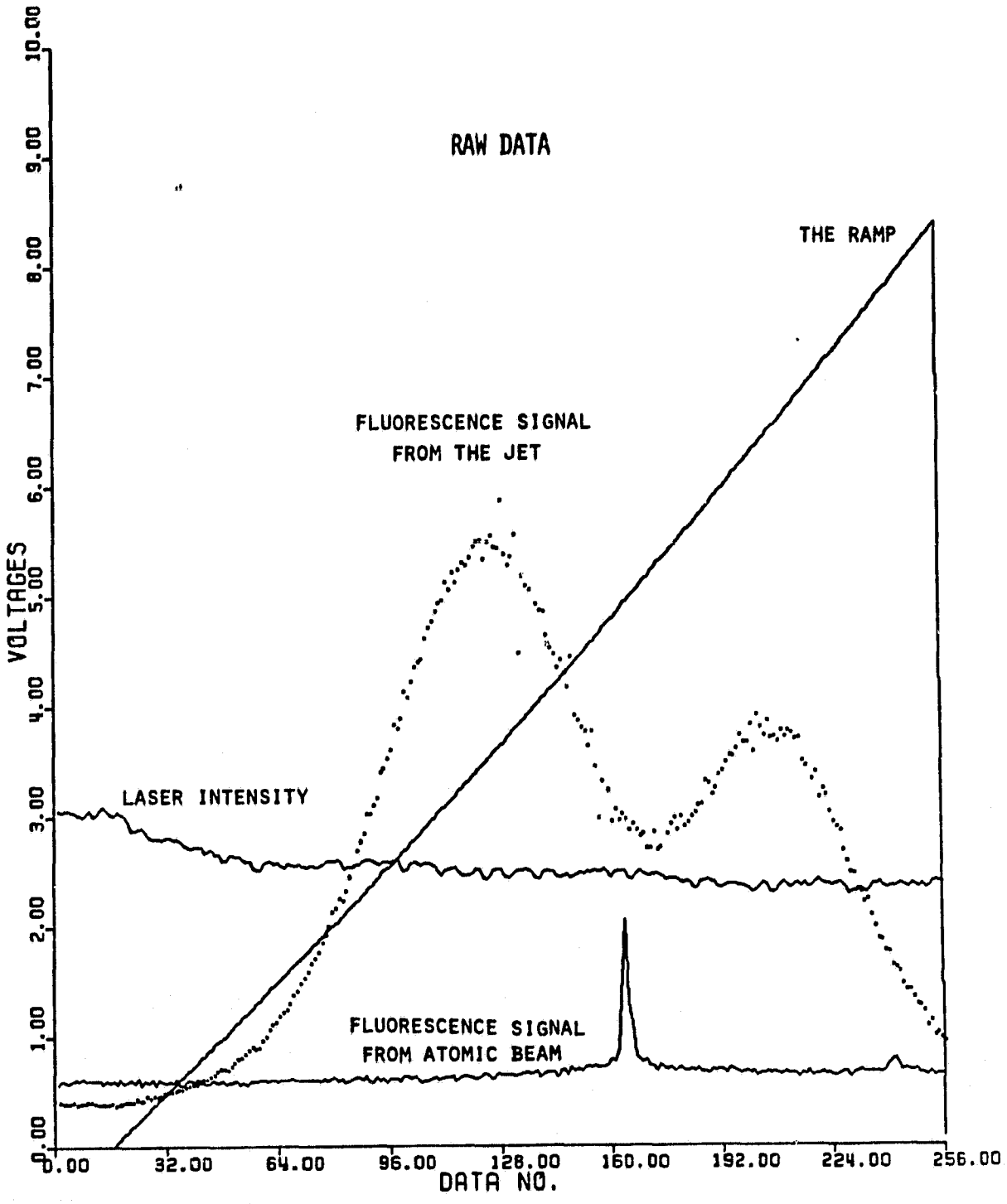

Figure 2. Raw data sampled by the computer. The ramp is the voltage applied to the piezoelectric crystal attached to one of the end mirrors of the dye laser cavity. Thus it can be converted into laser frequency.

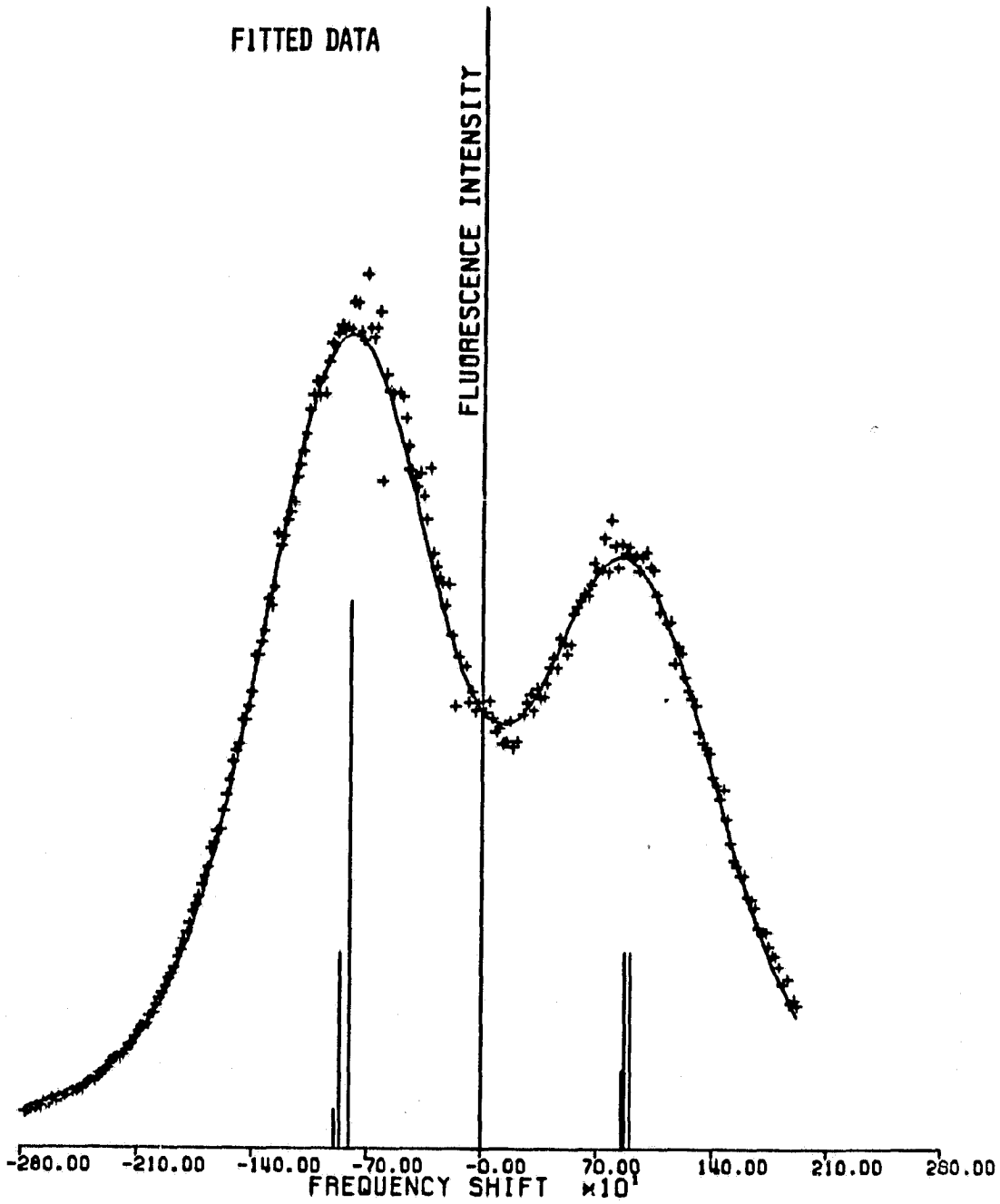

Figure 3. The Doppler shifted D_2 spectrum of sodium. The solid line is a theoretical fit to the experimental points represented by the crosses. The vertical bars indicate the hyperfine structure of the D_2 line.

ORIGINAL PAGE IS
OF POOR QUALITY

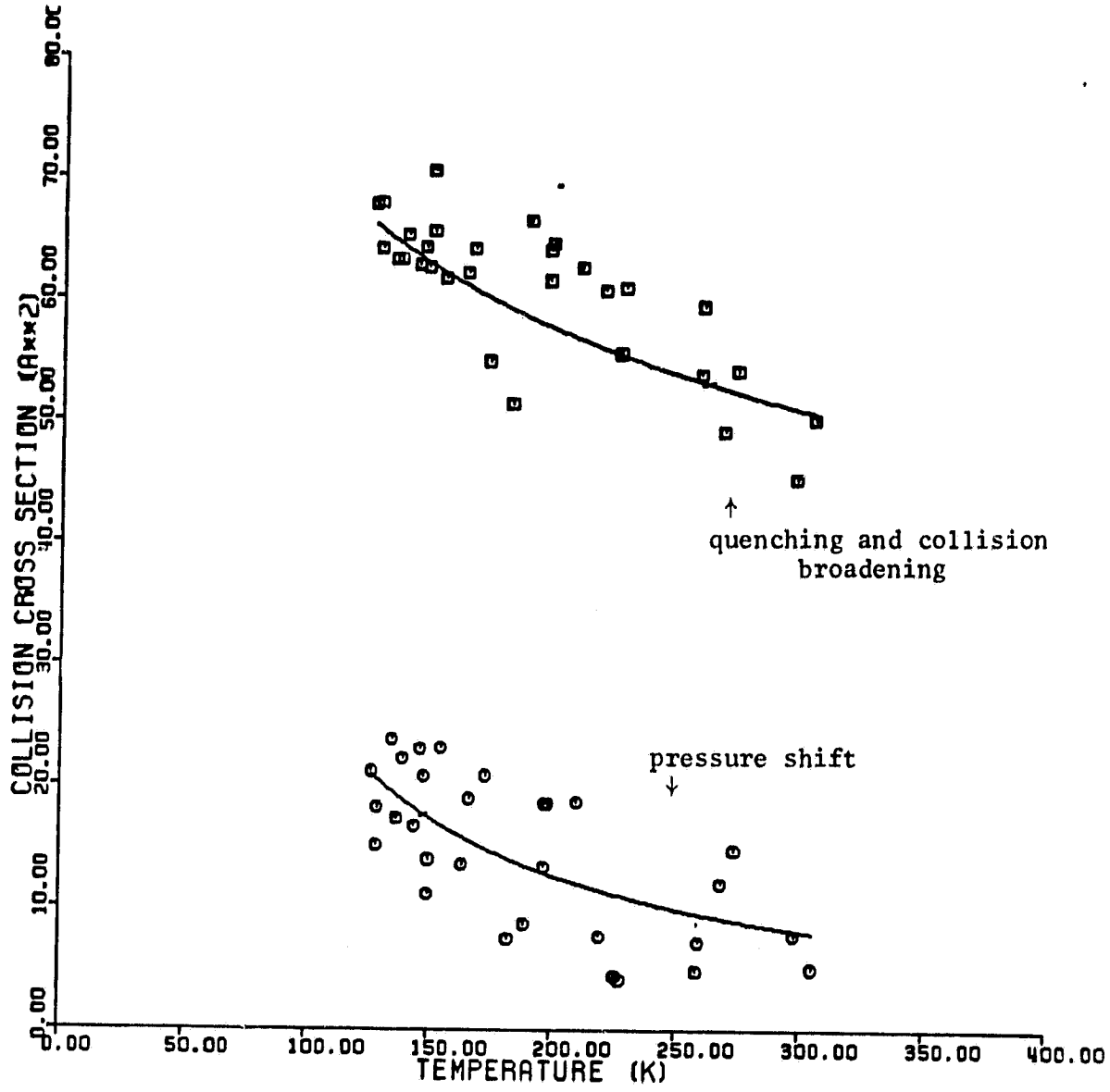

Figure 4. Temperature dependences of quenching and collision broadening cross section and pressure shift cross section. The solid lines are the least squares fitted curves.

ORIGINAL PAGE IS
OF POOR QUALITY

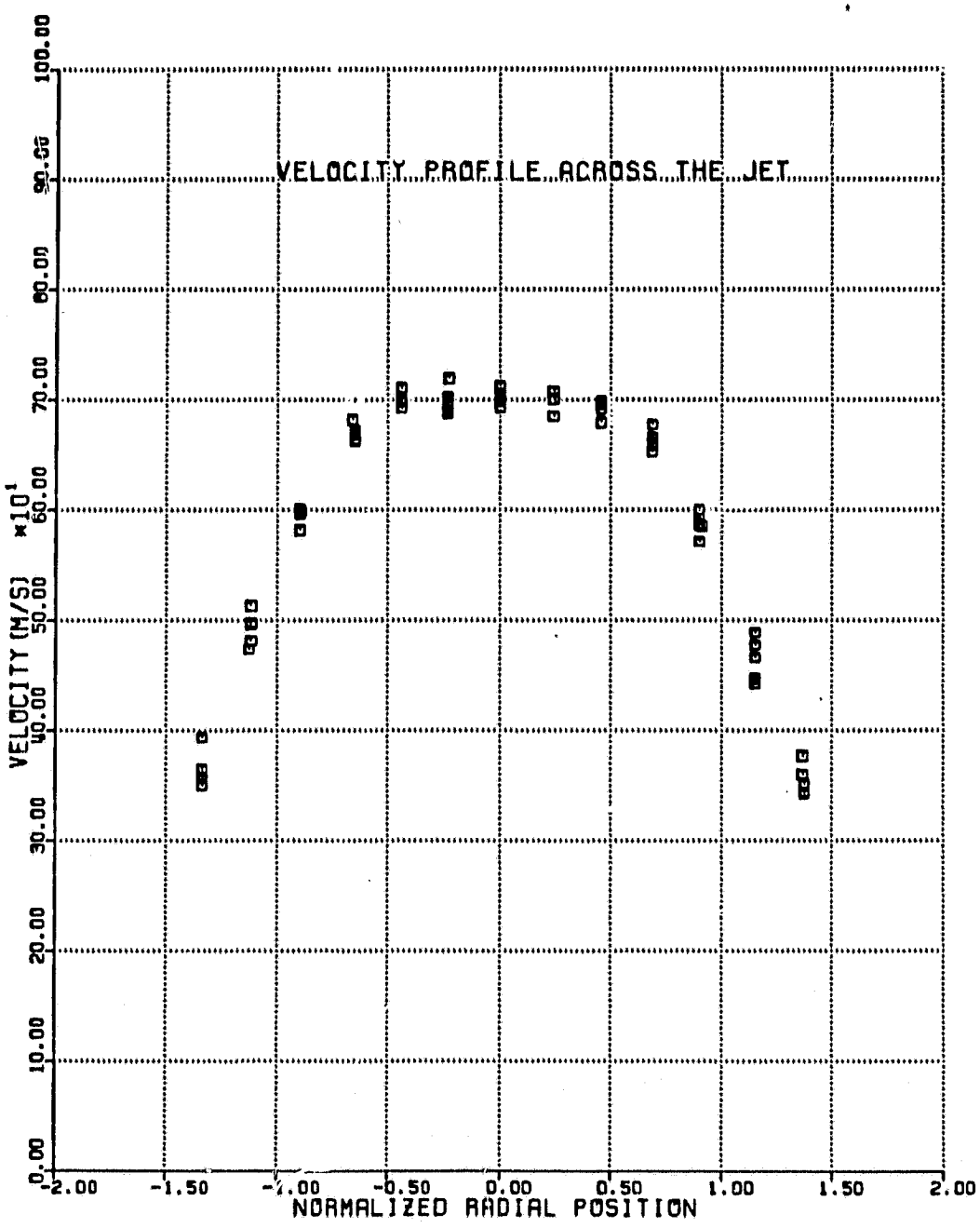

Figure 5. Velocity profile across an ideally expanded nitrogen jet measured with RDV.

ORIGINAL PAGE IS
OF POOR QUALITY

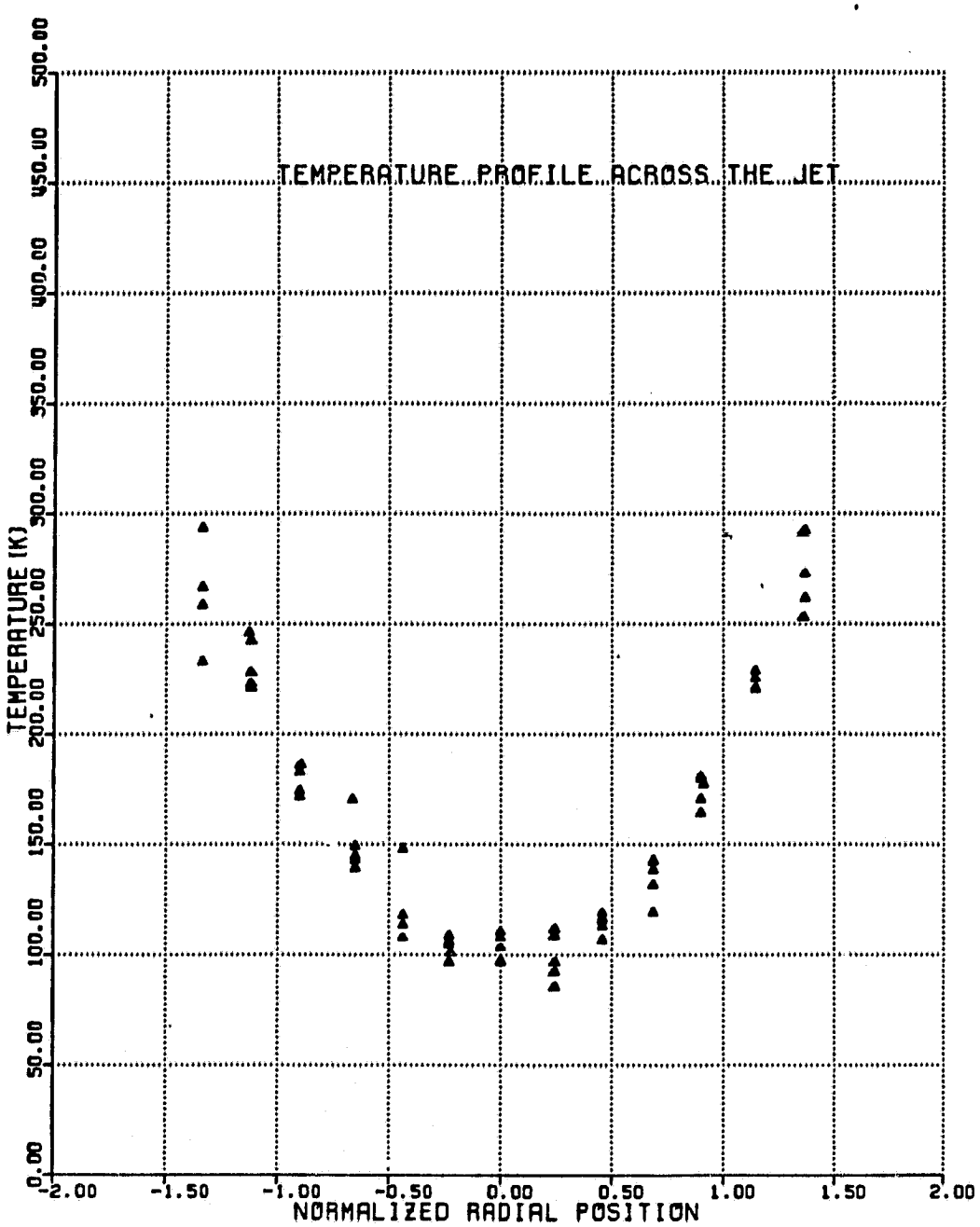

Figure 6. Static temperature profile across an ideally expanded nitrogen jet measured with RDV.

ORIGINAL PAGE IS
OF POOR QUALITY

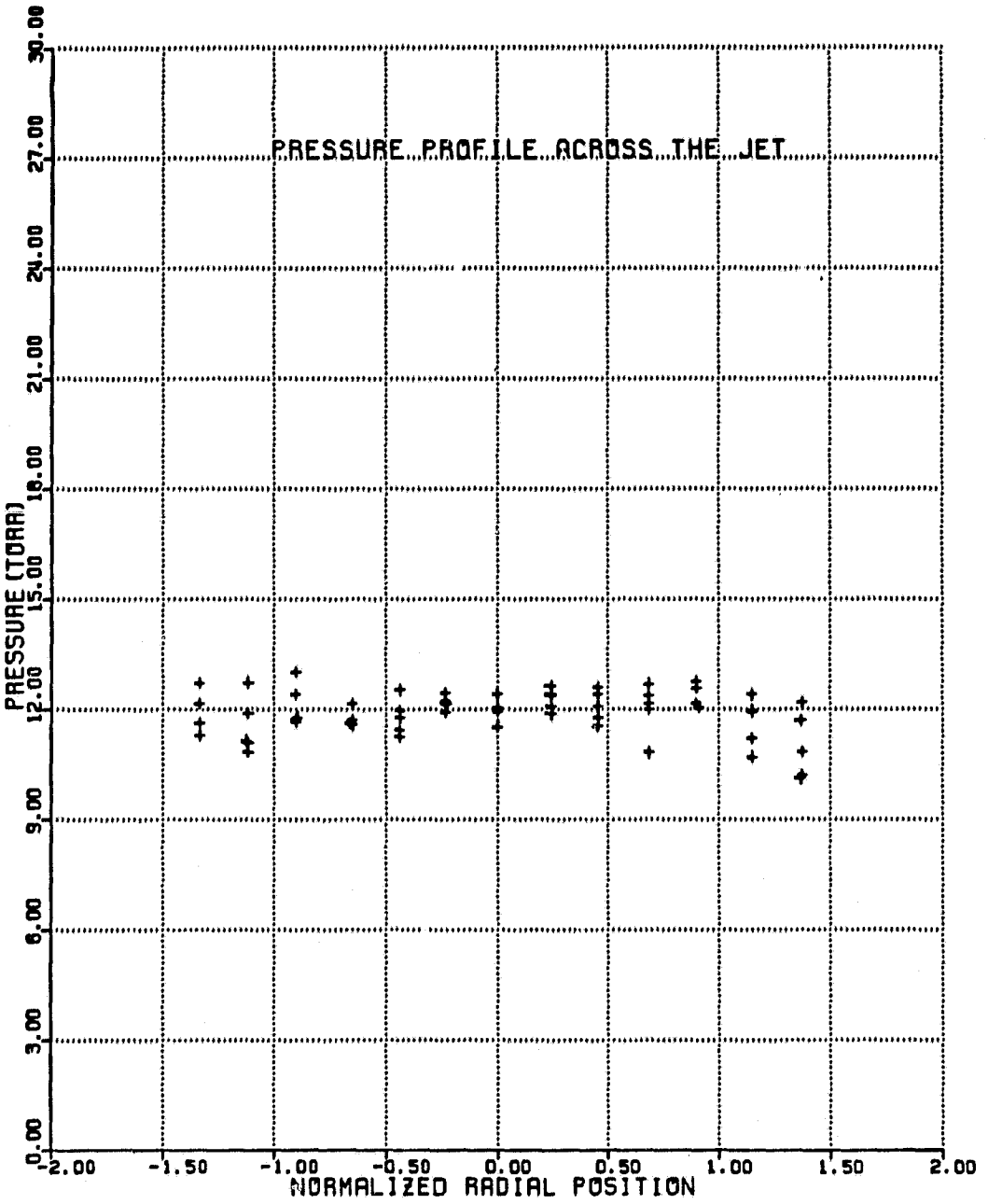

Figure 7. Static pressure profile across an ideally expanded nitrogen jet measured with RDV.

ORIGINAL PAGE IS
OF POOR QUALITY

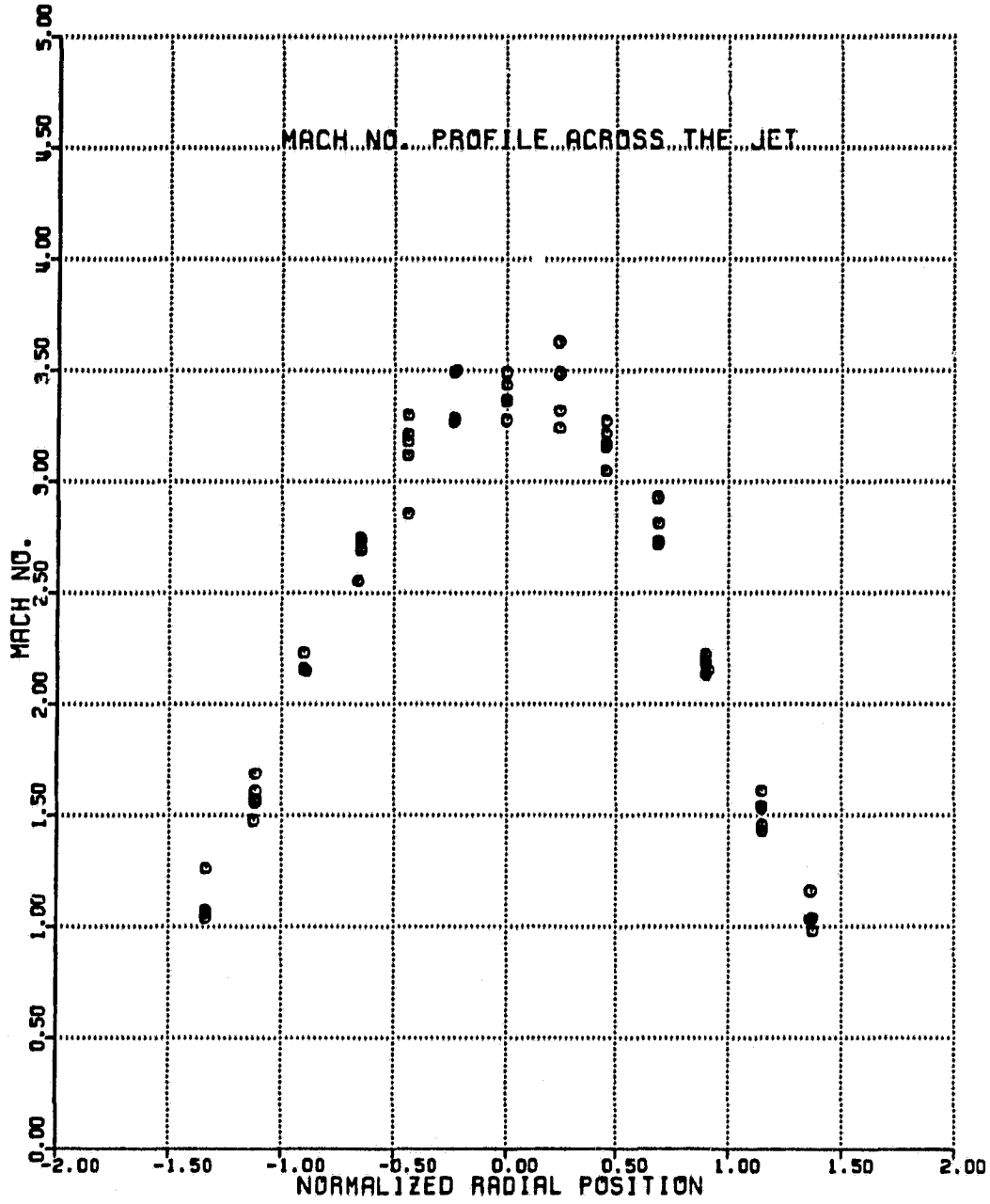

Figure 8. Mach number profile across an ideally expanded nitrogen jet measured with RDV.

ORIGINAL PAGE IS
OF POOR QUALITY

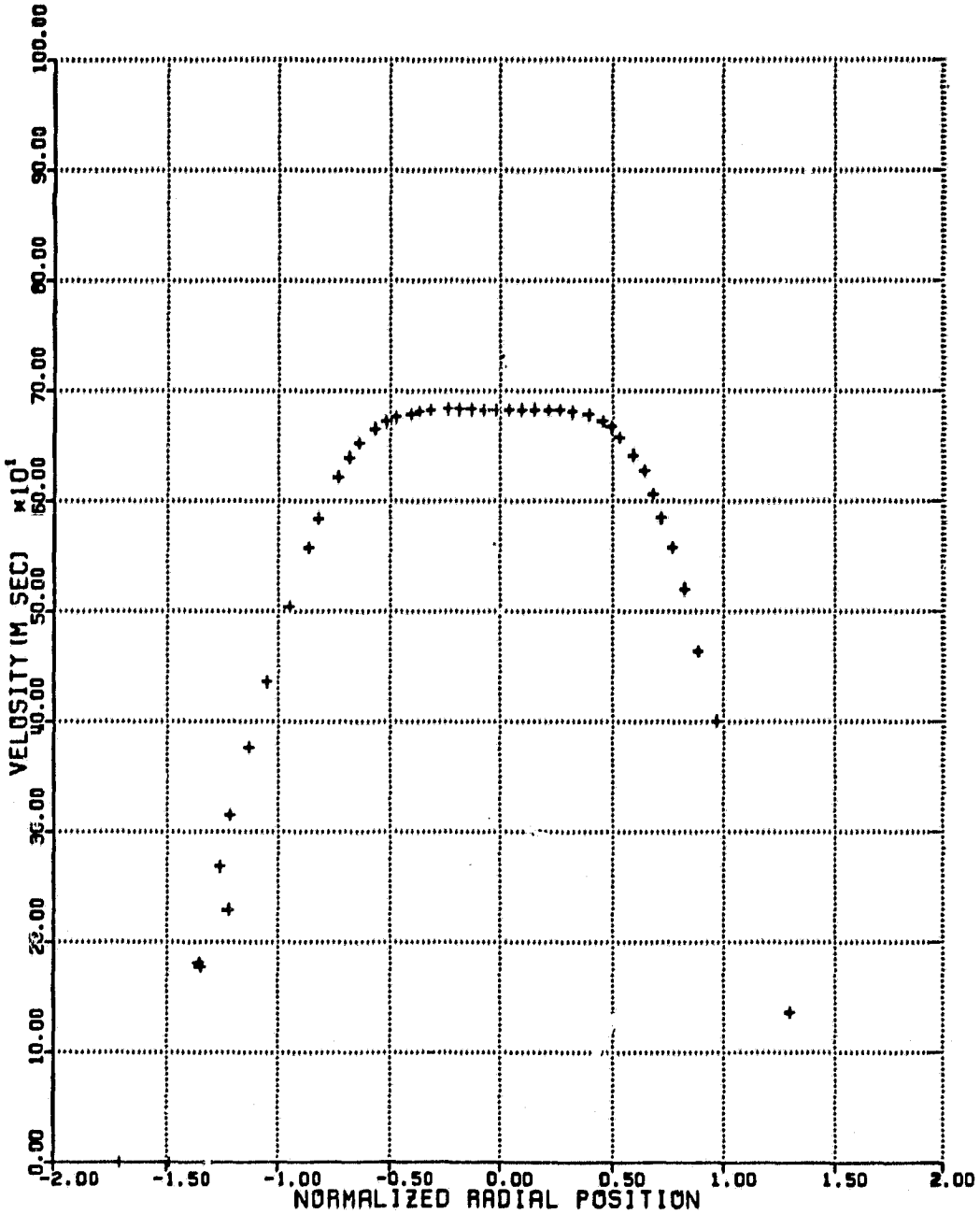

Figure 9. Velocity profile across an ideally expanded nitrogen jet. The velocities are calculated from the pitot pressures measured with a pitot probe.

ORIGINAL PAGE IS
OF POOR QUALITY

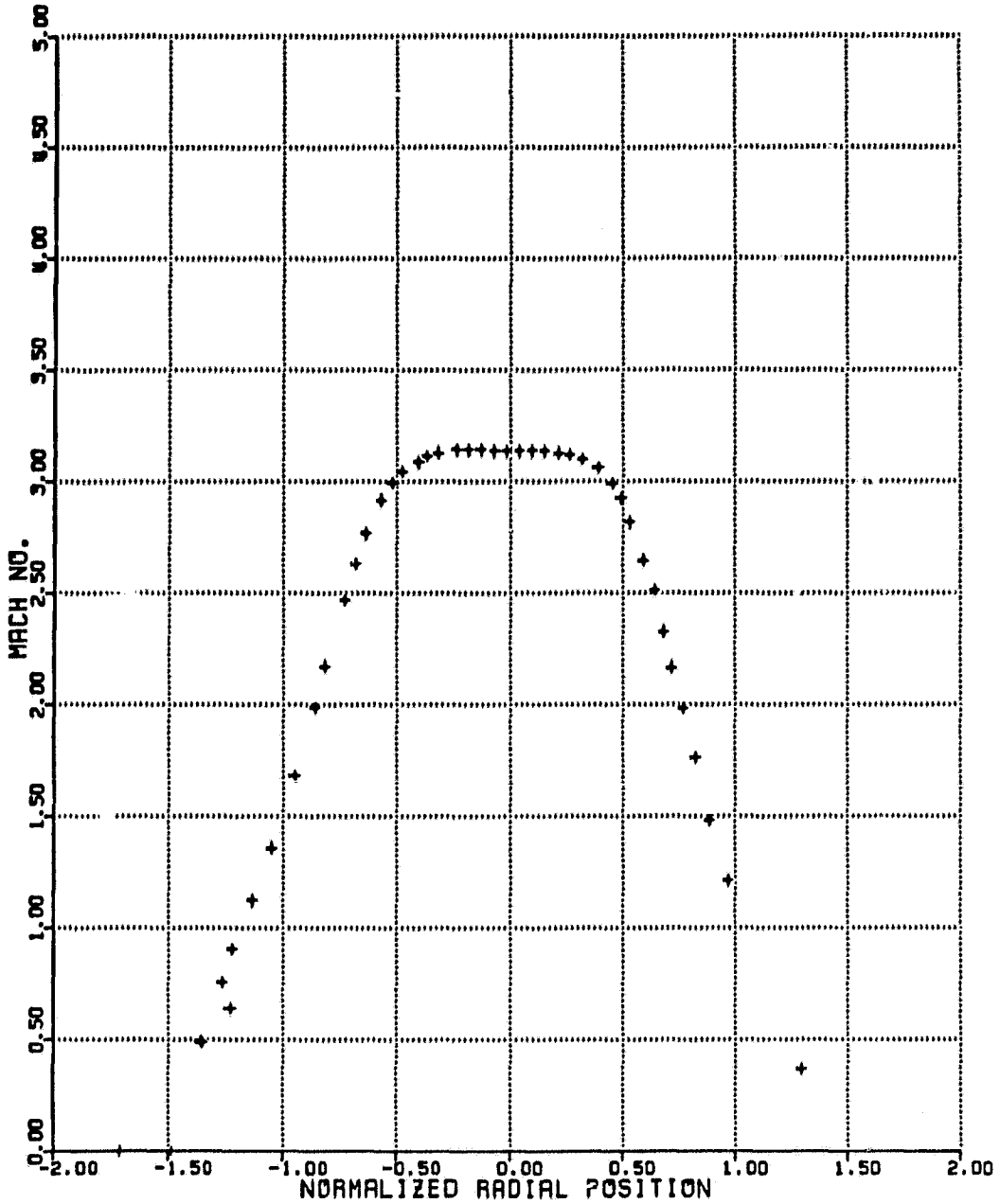

Figure 10. Mach number profile across an ideally expanded nitrogen jet. The Mach numbers are obtained from pitot pressures using the relation:

$$\frac{P_{static}}{P_{pitot}} = \frac{\left(\frac{2r}{r+1} M^2 - \frac{r-1}{r+1}\right)^{\frac{1}{r-1}}}{\left(\frac{r+1}{2} M^2\right)^{\frac{r}{(r-1)}}}$$

ORIGINAL PAGE IS
OF POOR QUALITY

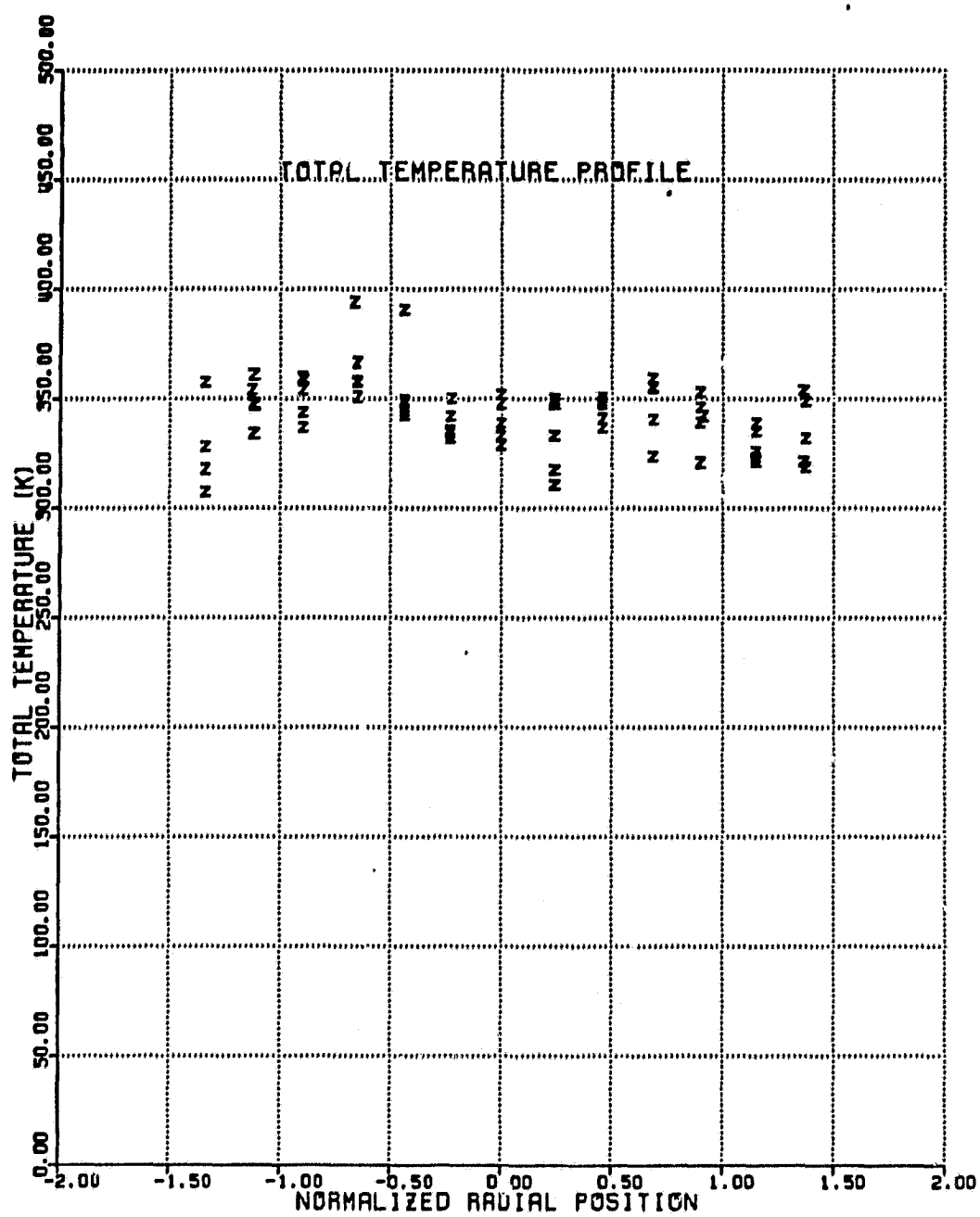

Figure 11. Total temperatore profile across an ideally expanded nitrogen jet. The total temperatures are calculated with the static temperatures and velocities measured with RDV.

ORIGINAL PAGE IS
OF POOR QUALITY

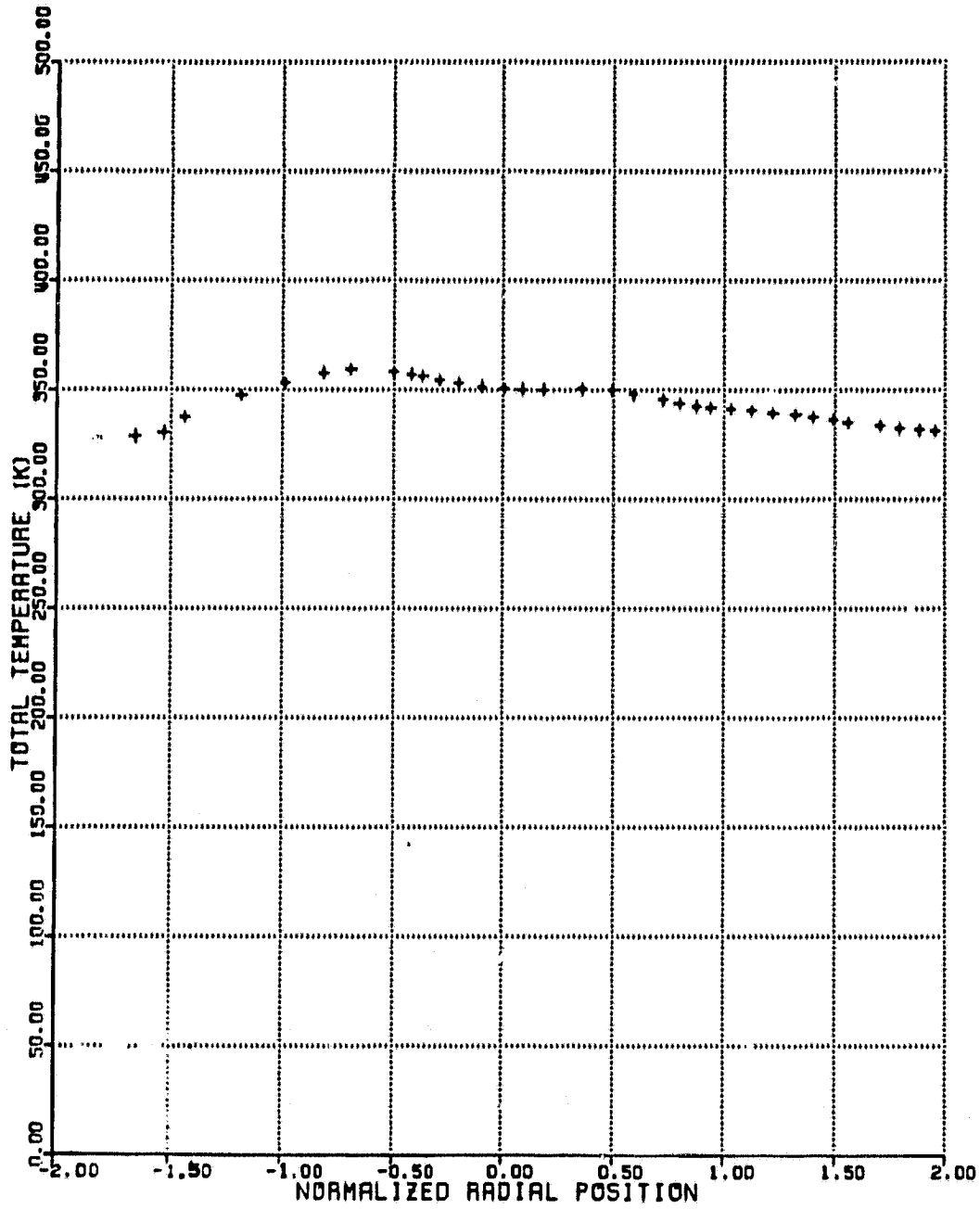

Figure 12. Total temperature profile across the jet measured with total temperature probe and corrected with a recovery coefficient of 0.95.

ORIGINAL PAGE IS
OF POOR QUALITY

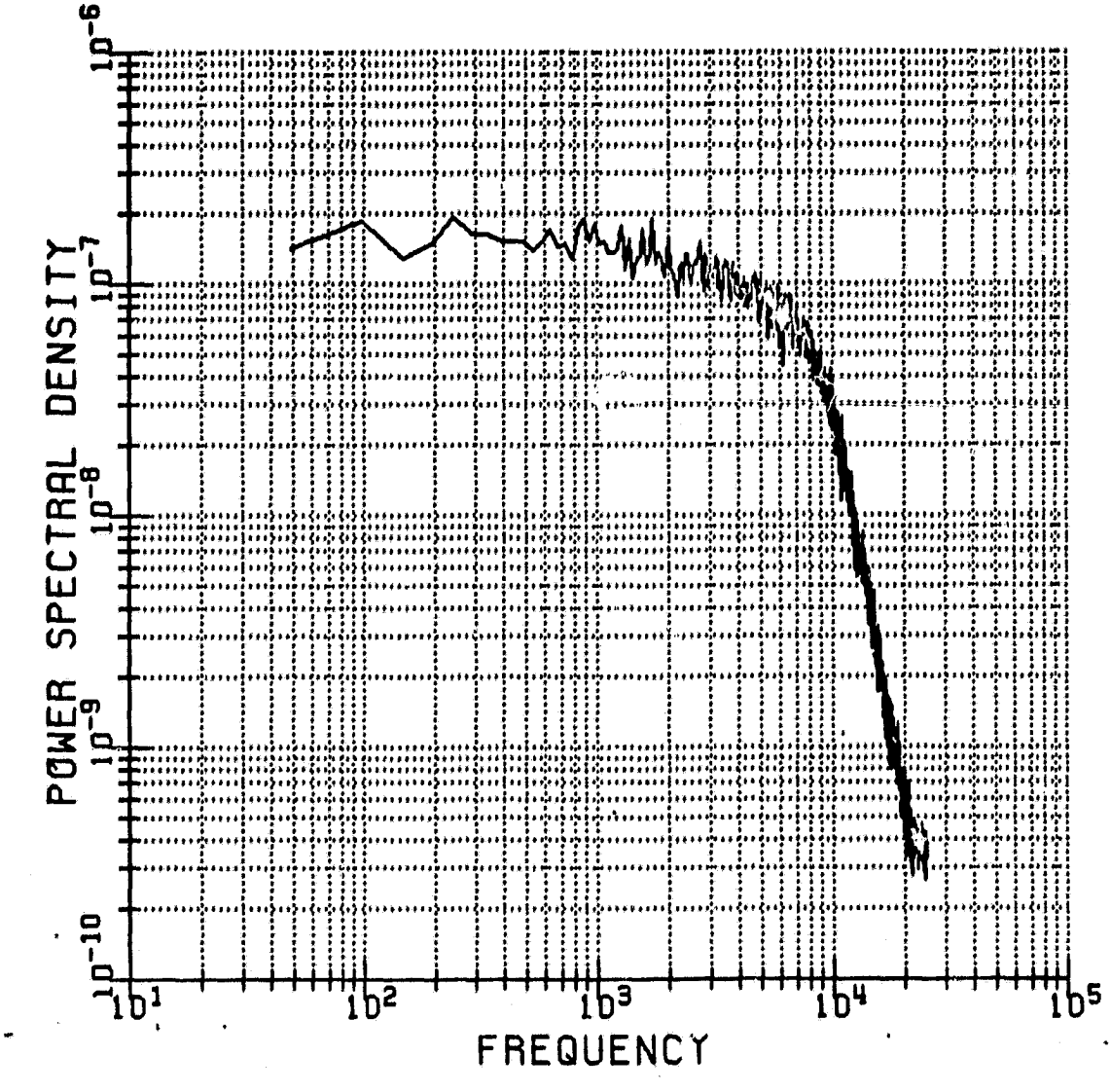

Figure 13. Power spectrum of the RDV signal from the free jet.

ORIGINAL PAGE IS
OF POOR QUALITY

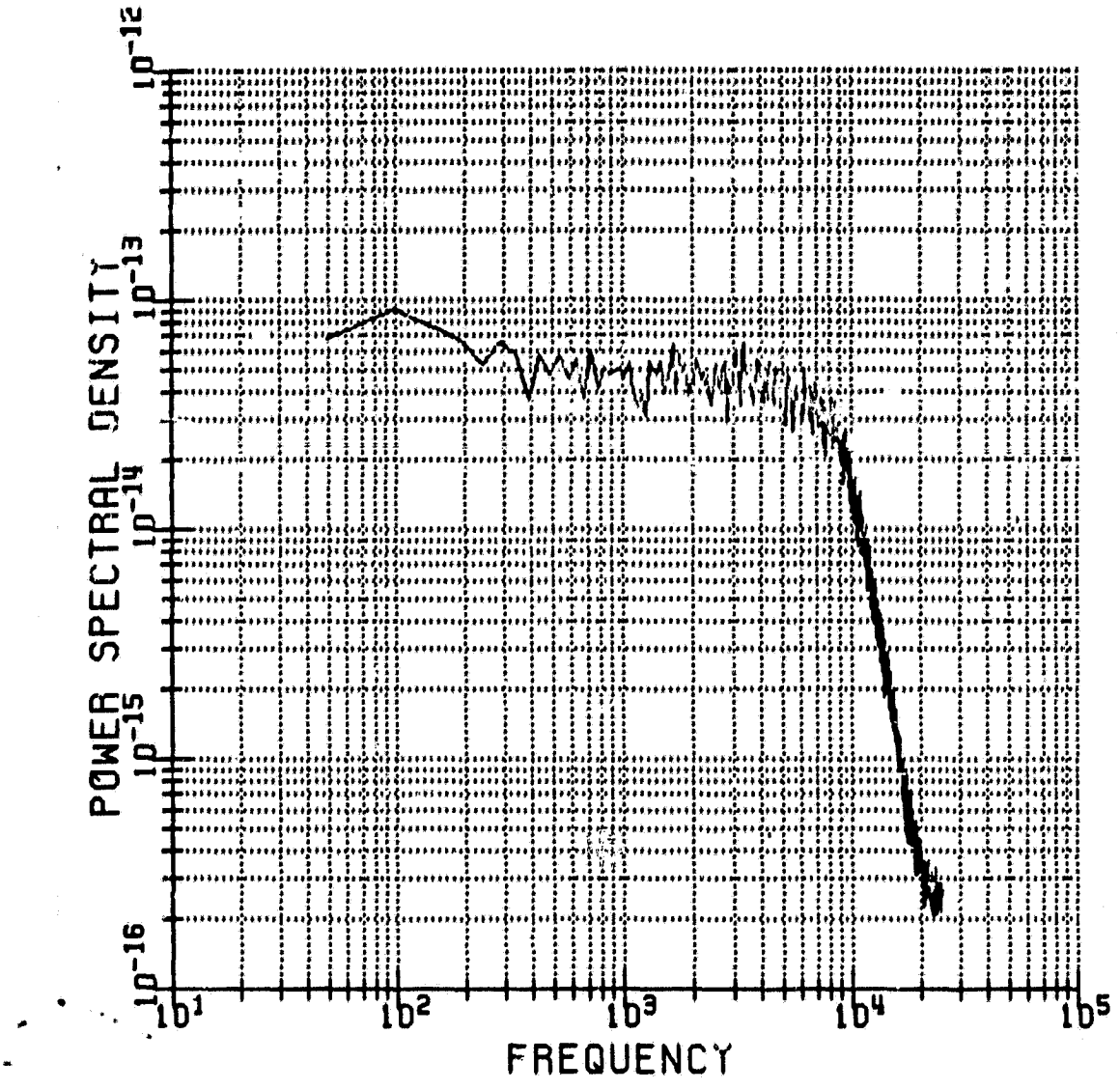

Figure 14. Power spectrum of the hot wire signal from the free jet.

ORIGINAL PAGE IS
OF POOR QUALITY

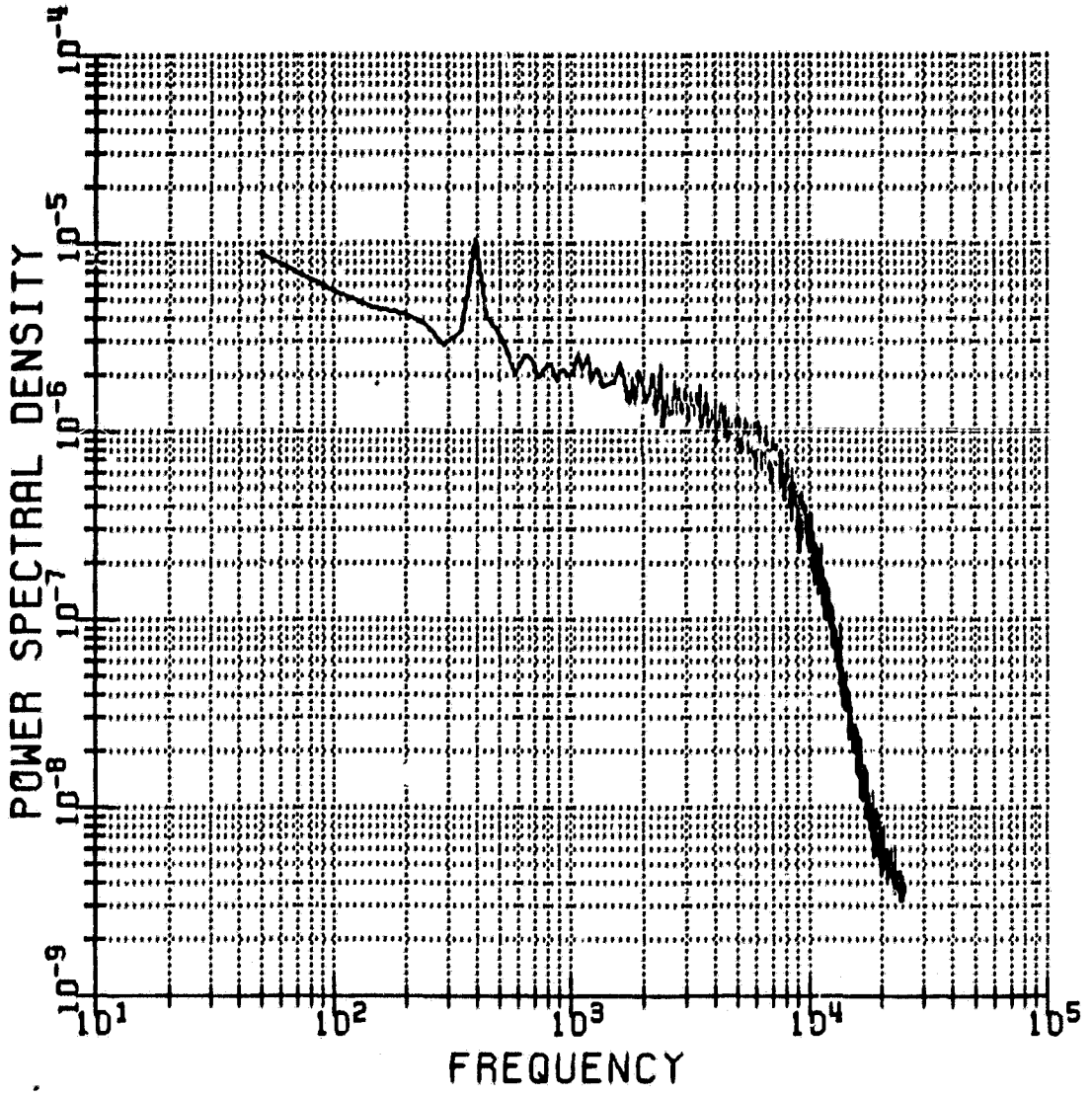

Figure 15. Power spectrum of the RDV signal from the jet with a small piece of metal in the flow.

ORIGINAL PAGE IS
OF POOR QUALITY

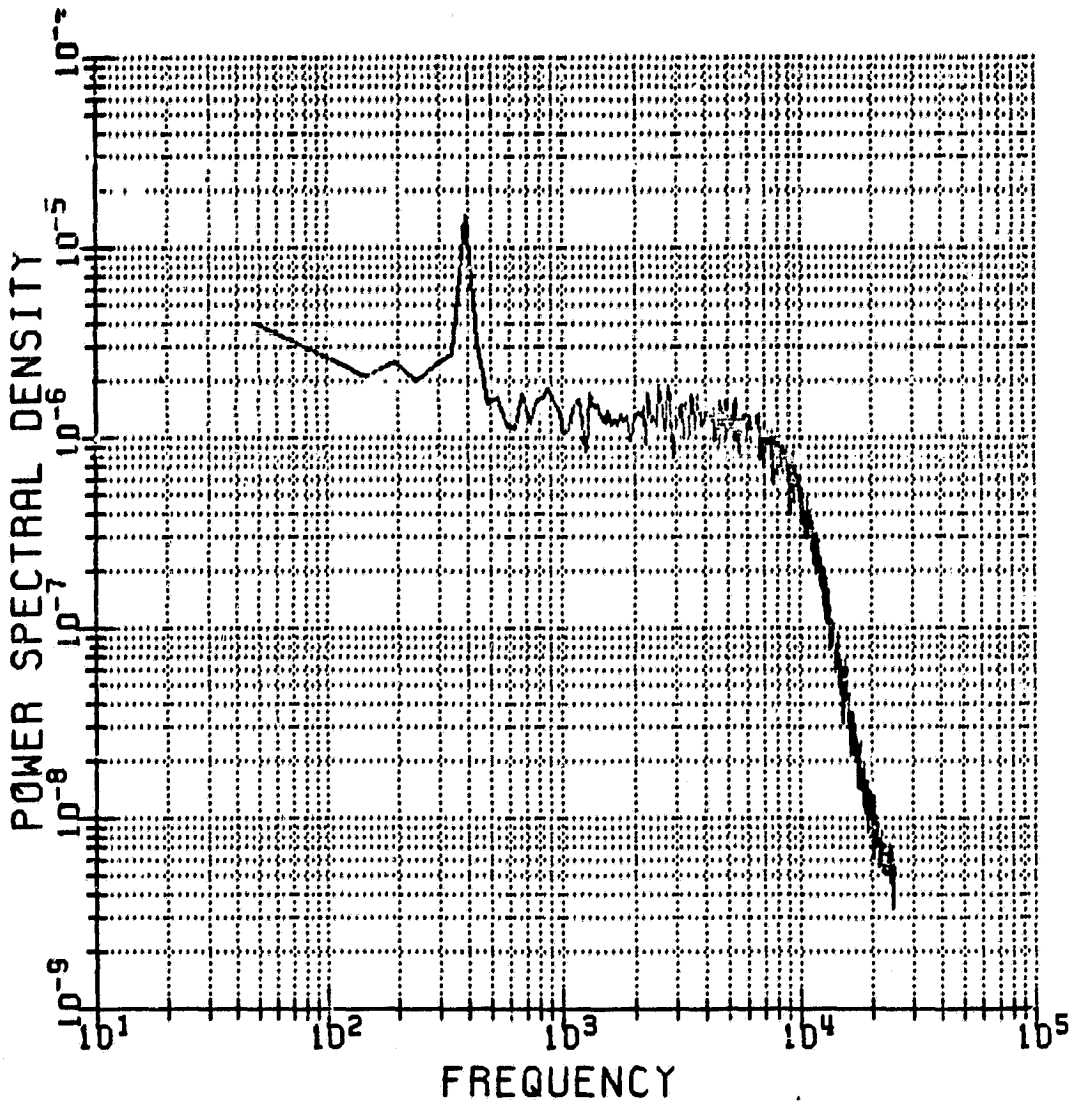

Figure 16. Power spectrum of the hot wire signal from the jet with a small piece of metal in the flow.

ORIGINAL PAGE IS
OF POOR QUALITY

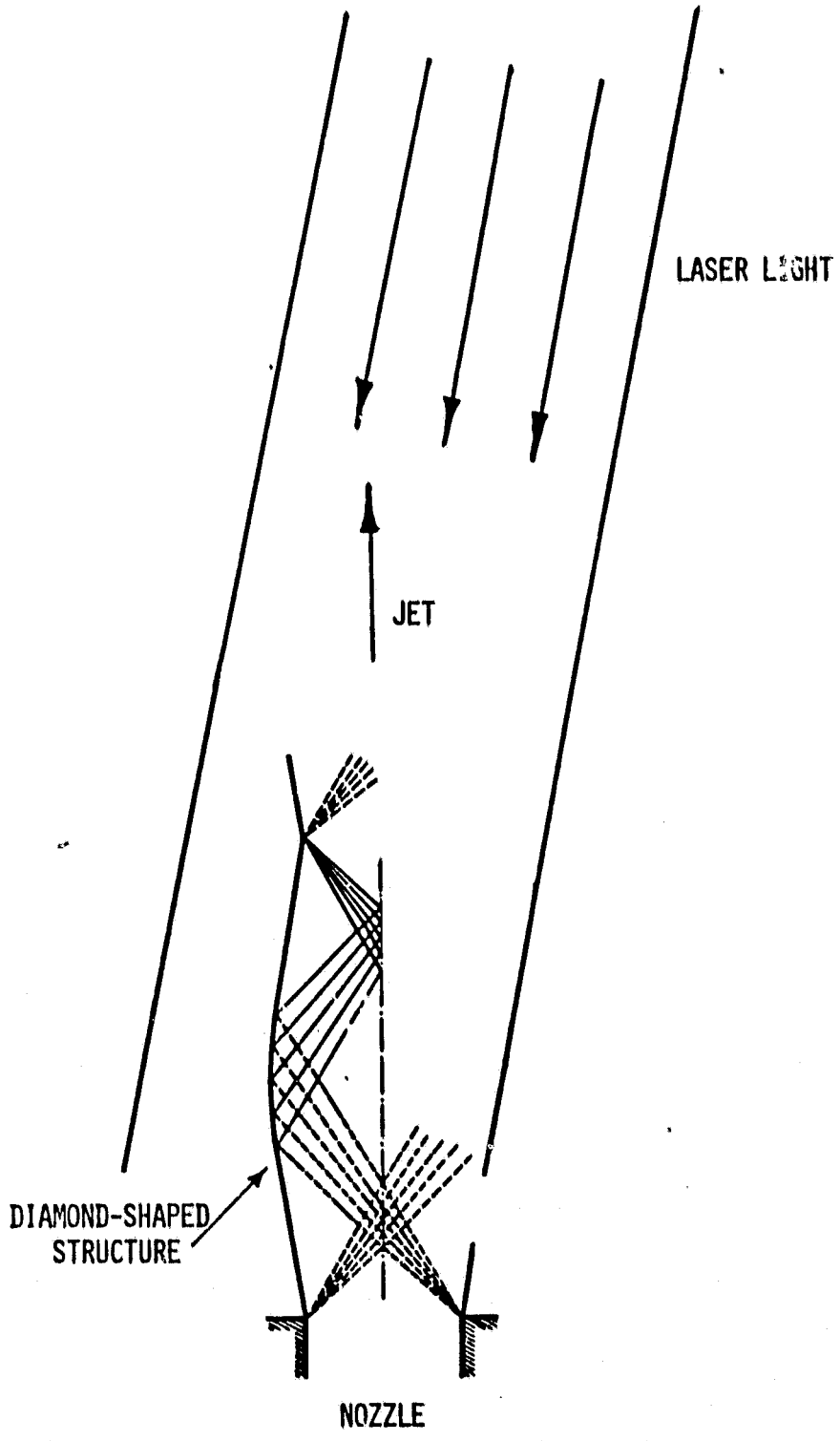

Figure 17. Configuration for flow visualization in an underexpanded nitrogen jet.

ORIGINAL PAGE
BLACK AND WHITE PHOTOGRAPH

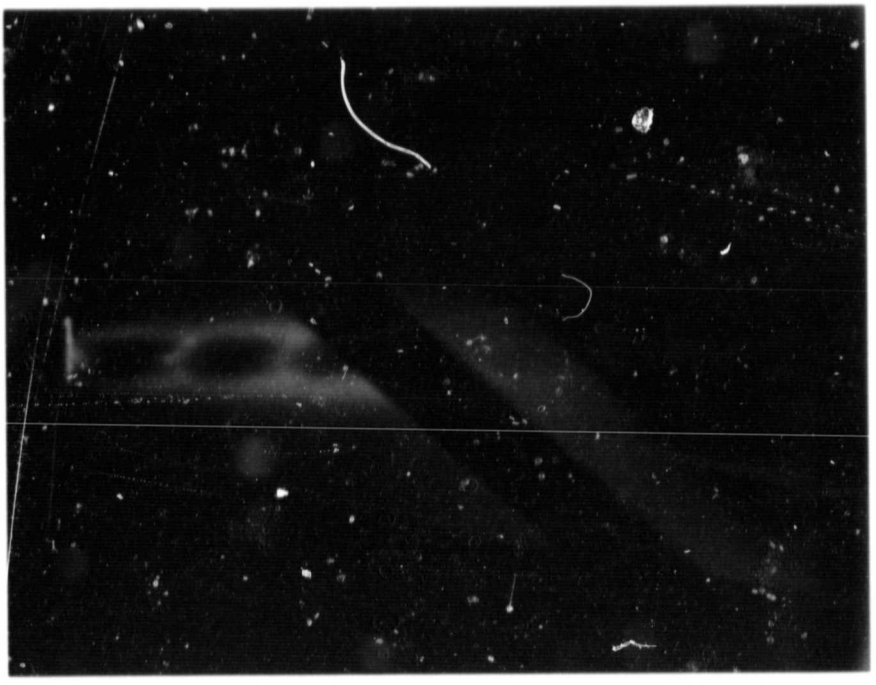

Figure 18. Flow visualization with the laser focused to a narrow sheet of light and tuned to highlight low velocity components. The diamond shaped structure of an underexpanded jet can be seen in the photograph. The narrow region downstream shows fluorescence from an unfocused laser. Here the structure is washed out

ORIGINAL PAGE
BLACK AND WHITE PHOTOGRAPH

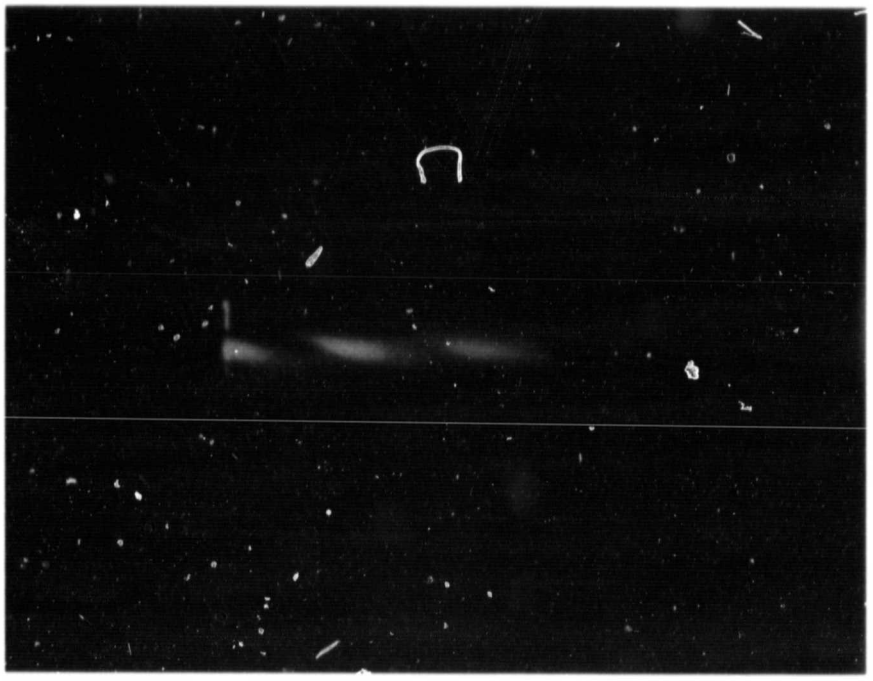

Figure 19. Flow visualization of the same jet as shown in Figure 14 except with the laser focused to a narrow sheet and tuned to highlight high velocity components.